SECOND EUROPEAN CONFERENCE ON EARTHQUAKE ENGINEERING
AND SEISMOLOGY, ISTANBUL AUG. 25-29, 2014

RECORD-TO-RECORD VARIABILITY OF THE COLLAPSE CAPACITY OF MULTI-STORY FRAME STRUCTURES VULNERABLE TO P-DELTA

Christoph ADAM[1], Styliani TSANTAKI[2], Luis F. IBARRA[3] and David KAMPENHUBER[4]

ABSTRACT

In this paper the record-to-record variability of the collapse capacity of highly inelastic multi-story frame structures is evaluated. These frames are vulnerable to the destabilizing effect of gravity loads (P-delta effect). In particular, the effect of different spectral pseudo-acceleration based intensity measures (IMs) at target periods, or alternatively, averaged over a certain period range is evaluated. In a parametric study on generic frame structures characteristic specific structural parameters are varied to quantify their impact on the collapse capacity dispersion. From the results it can be concluded that it should be strictly distinguished between single-degree-of-freedom (SDOF) and multi-degree-of-freedom (MDOF) structures when selecting the underlying IM for the definition of the collapse capacity. For MDOF structures consideration of higher modes in the IM leads to the smallest dispersion. In a SDOF system, however, an averaged intensity measure including periods below the system period increases the RTR variability of the collapse capacity.

INTRODUCTION

The seismic response dispersion due to record-to-record (RTR) uncertainties depends on various factors such as the set of earthquake ground motions, the considered response quantity, the limit state, the type of structure (e.g., regularity), and the intensity measure (IM). In this paper, the effect of different IMs on the RTR variability of the seismic collapse capacity of multi-story moment-resisting frames vulnerable to the destabilizing effect of gravity loads (i.e., global P-delta effect), where material deterioration is negligible, is investigated.

Since there is no unique definition of intensity of an earthquake record, several IMs have been proposed, such as elastic ground motion based scalar IMs (e.g., peak ground acceleration (PGA), peak ground velocity (PGV), peak ground displacement (PGD)), and elastic and inelastic spectral based IMs (e.g., spectral acceleration and spectral displacement at the fundamental period of the structure). Other IMs include spectral values related to higher mode effects or period elongation (Cordova et al., 2001; Luco and Cornell, 2007; Kadas et al., 2011), and vector valued IMs (e.g., Baker and Cornell, 2005). Although many advanced IMs have been proposed, there are still a few limitations such as the derivation of attenuation relations, the selection of the spectral values in case of higher mode and period elongation incorporation, their validation for several structural systems, etc. Based on information theory concepts, Jalayer et al. (2012) compared some commonly used IMs. The

[1] Professor, Unit of Applied Mechanics, University of Innsbruck, Austria, christoph.adam@uibk.ac.at
[2] Dipl.-Ing., Unit of Applied Mechanics, University of Innsbruck, Austria, styliani.tsantaki@uibk.ac.at
[3] Assistant Professor, Department of Civil and Environmental Engineering, University of Utah, U.S.A., luis.ibarra@utah.edu
[4] Dipl.-Ing., Unit of Applied Mechanics, University of Innsbruck, Austria, david.kampenhuber@uibk.ac.at

importance of the spectral shape consideration has been clearly demonstrated by Baker and Cornell (2006). Haselton (2009) evaluated several ground motion selection and modification methods utilizing a point of comparison methodology, estimating the true response. However, most of these studies do not focus on the collapse limit state.

The IMs used in this study are the spectral pseudo-acceleration at the fundamental period with and without considering gravity loads, and the geometric mean of the pseudo-acceleration over a specific period range depending on the fundamental period. Four sets of P-delta vulnerable generic frames are developed varying the number of stories, the elastic fundamental period, and the global negative post-yield stiffness ratio obtained from a first mode pushover analysis. In a parametric study, the RTR dispersion of the collapse capacity using the records of a ground motion set is derived, and the effect of the IM on the RTR variability is evaluated.

FRAMEWORK OF THE PRESENT STUDY

Collapse of frame structures vulnerable to P-delta

During severe seismic excitations inelastic deformations combined with gravity may cause a structure to approach a state of dynamic instability. A first mode pushover analysis delivers strong evidence for the vulnerability of a regular multi-story frame to P-delta induced global seismic collapse (Adam and Jäger, 2012). For instance, the black curve of Figure 1 illustrates the global pushover curve of a flexible structure, where the base shear V is plotted against the roof displacement x_N, disregarding the gravity loads in the nonlinear static analysis. The red pushover curve considers gravity loads, which lead to a negative post-yield stiffness due to the P-delta effect. When severe seismic excitation drives this structure into its inelastic branch of deformation, a state of dynamic instability may be approached, and the global collapse limit state is attained at a rapid rate. The global pushover curves of a multi-degree-of-freedom (MDOF) structure do not exhibit a uniform stability coefficient in the entire range of elastic and inelastic deformations such as in a single-degree-of-freedom (SDOF) system (MacRae, 1994). As observed in Figure 1, two stability coefficients can be identified in a bilinear approximation of pushover curves with and without P-delta effect. That is, a stability coefficient in the elastic range of deformation (θ_e) and a stability coefficient in the post-yield range of deformation (θ_i). According to Medina and Krawinkler (2003) θ_i can be much larger than θ_e: $\theta_i > (>) \theta_e$. When predicting the collapse capacity of a flexible structure, in many cases cyclic deterioration of the structural components can be disregarded. In those cases, a precondition for seismic collapse is that the post-yield tangent stiffness is negative, or alternatively expressed, the difference of inelastic stability coefficient θ_i and global hardening ratio α_s is larger than zero, i.e., $\theta_i - \alpha_s > 0$, compare with Figure 1. For instance, Adam and Jäger (2012) introduced the collapse capacity spectrum method for simplified assessment of the collapse capacity of highly inelastic multi-story frame structures, where material deterioration can be neglected.

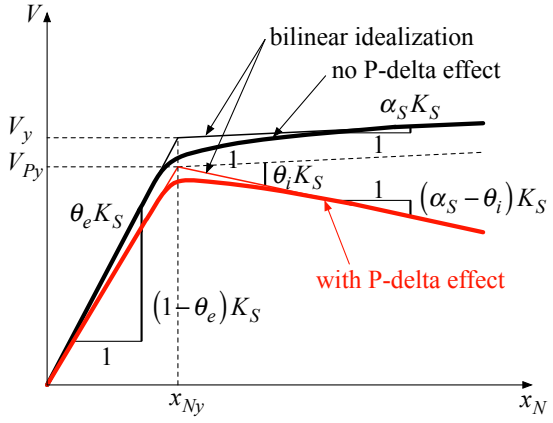

Figure 1. Global pushover curve of a multi-story frame structure vulnerable to the P-delta effect (red curve), and the corresponding outcome disregarding gravity loads (black curve)

Collapse capacity and its record-to-record variability

The collapse capacity is defined as the maximum ground motion intensity at which the structure still maintains dynamic stability (Krawinkler et al., 2009). Generally the Incremental Dynamic Analysis (IDA) procedure is used to predict collapse capacity. An IDA consists of a series of time history analysis, in which the intensity of a particular ground motion is monotonically increased. As a result, the IM is plotted against a characteristic response quantity, such as the story drift or roof drift. The procedure is stopped when the evaluated response quantity grows unbounded, indicating that structural failure occurs. The corresponding IM is referred to as the structural collapse capacity subjected to that particular ground motion record. In many cases the IM is an acceleration quantity such as the PGA, or more commonly, the 5% spectral acceleration at the fundamental elastic period of the structure ($S_a(T_1)$). In such a case it is beneficial to define the relative collapse capacity according to

$$CC_i\big|_{IM} = \frac{IM_i\big|_{collapse}}{g\gamma} \tag{1}$$

where γ is the base shear yield coefficient, i.e., the ratio of the base shear at yield V_y to the effective weight W of the structure: $\gamma = V_y / W$, and g is the acceleration gravity. Subscript i denotes the underlying ground motion record characterized through IM with dimension acceleration, $IM_i\big|_{collapse}$. The relative collapse capacity CC_i is non-dimensional, and thus, it provides information for a larger class of structures capturing different base shear yield coefficients.

Since the collapse capacity is highly record dependent, it is derived for the ground motion records of a record set and statistically evaluated. Shome and Cornell (1999) and Ibarra and Krawinkler (2011) provide good arguments for representing a set of corresponding collapse capacities by a log-normal distribution, which is characterized by the median $\mu_{\ln CC}$ of the natural logarithm of individual collapse capacities and the standard deviation β of the logarithm of individual collapse capacities (FEMA-350, 2000):

$$\beta = \sqrt{\sum_{i=1}^{r} \frac{(\ln CC_i - \mu_{\ln CC})^2}{r-1}} \tag{2}$$

In Equation 2 r is the total number of individual collapse capacities, CC_i, $i = 1,...,r$, and thus the number of utilized ground motion records.

Case study intensity measures

In this paper, the choice of an appropriate IM for defining the collapse capacity of moment-resisting frames vulnerable to the P-delta effect is investigated. For this purpose, RTR uncertainties of the collapse capacity are captured employing the 44 far-field ground motions of the FEMA P-695-FF record set, also known as ATC63-FF set (FEMA P-695, 2009). The records of the FEMA P-695-FF set originate from seismic events of magnitude between 6.5 and 7.6 and closest distance to the fault rupture larger than 10 km. Thereby, only strike-slip and reverse sources are considered. The 44 records of this set were recorded on NEHRP site classes C (soft rock) and D (stiff soil). This ground motion set has a constant mean epsilon value of about 0.6 for code defined periods less or equal to 0.5 s, linearly decreasing positive mean values as the period increases and nearly zero mean epsilon values for periods larger or equal to 1.5 s.

According to Bianchini et al. (2009) an appropriate IM should comply with the following properties:

- Hazard compatibility, i.e. the IM quantifies appropriately the ground motion hazard at the site,
- efficiency, which is defined as the dispersion of the IM values associated with a given response quantity level,
- sufficiency, i.e. the IM is conditionally statistically independent of ground motion characteristics such as magnitude, distance, epsilon, etc., and
- scaling robustness.

In the present study, the efficiency of four different IMs at collapse of P-delta vulnerable MDOF frame structures is assessed. In particular, these are the following IMs:

- The 5% damped spectral pseudo-acceleration $S_a(T_1)$ at the fundamental period of the structure without considering P-delta T_1 serves as the benchmark IM.
- Alternatively, the 5% damped spectral pseudo-acceleration $S_a(T_1^{P\Delta})$ at the fundamental period of vibration of the system in the presence of gravity loads $T_1^{P\Delta}$ is utilized.
- The "average" IM $S_{a,gm}(T_1,1.6T_1)$, which combines the 5% damped spectral pseudo accelerations in the period band between the fundamental period and 1.6 times the fundamental structural period, accounts for period elongation due to inelasticity.
- The "average" IM $S_{a,gm}(0.2T_1,1.6T_1)$ accounts both for period elongation due to inelasticity and for higher mode effects.

The "average" IMs $S_{a,gm}$ are a slightly modified form of an "average" IM as defined in Bianchini et al. (2009). They are both based on the geometric mean of the 5% damped spectral pseudo-accelerations S_a over the period range ΔT,

$$\Delta T = T^{(n)} - T^{(1)}, \quad T^{(n)} > T^{(1)} \tag{3}$$

between a lower bound period $T^{(1)}$ and an elongated period $T^{(n)}$ larger than $T^{(1)}$. In contrast to Bianchini et al. (2009), where S_a is read at 10 log-spaced periods within ΔT, in Tsantaki and Adam (2013) at equally spaced discrete periods $T^{(i)}$ within ΔT,

$$T^{(i)} = T^{(1)} + \left(i-1\right)\delta T, \quad i = 1,...,n \quad , \quad \delta T = \frac{\Delta T}{n-1} = \frac{T^{(n)} - T^{(1)}}{n-1} \tag{4}$$

The corresponding discrete 5%-damped spectral pseudo-accelerations $S_a(T^{(i)})$ $(i = 1,...,n)$ are combined as proposed in Bianchini et al. (2009):

$$S_{a,gm}(T^{(1)},...,T^{(i)},...,T^{(n)}) = \left(\prod_{i=1}^{n} S_a(T^{(i)}) \right)^{1/n} \tag{5}$$

It is noted that $T^{(i)}$ is the *i*th period in the set of *n* periods $T^{(1)},...,T^{(i)},...,T^{(n)}$ but in general not the fundamental system period T_1. In Bianchini et al. (2009) it is shown that $S_{a,gm}(T^{(1)},...,T^{(i)},...,T^{(n)})$, or briefly $S_{a,gm}(T^{(1)},T^{(n)})$, satisfies the hazard compatibility property, and moreover, it is statistically independent from ground motion characteristics and scaling factors, thus complying with the IM properties sufficiency and scaling robustness.

Based on parametric IDAs on P-delta vulnerable highly inelastic SDOF systems, Tsantaki and Adam (2013) found that the upper elongated period $T^{(n)}$ leading to the minimum RTR dispersion of the collapse capacity is around $1.6T_{SDOF}$, fluctuating in the range between $1.4T_{SDOF}$ and $2.0T_{SDOF}$. According to this study, for these SDOF systems the "optimal" lower bound period $T^{(1)}$ corresponds to the elastic period, i.e., $T^{(1)} = T_{SDOF}$. The reduction of the RTR dispersion of the collapse capacity of SDOF systems based on this IM $S_{a,gm}(T_{SDOF},1.6T_{SDOF})$ compared to the results for the common IM $S_a(T_{SDOF})$ is up to 50% (Tsantaki and Adam, 2013). Exemplarily, Figure 2 shows dispersion measure β of the collapse capacity for the conventional IM $S_a(T_{SDOF})$ and the IM $S_{a,gm}(T_{SDOF},1.6T_{SDOF})$ for two different negative post-yield stiffness ratios equal to 0.20 and 0.40, respectively, plotted against the elastic system period T_{SDOF}. These examples visualize the enhanced efficiency of the average IM.

However, numerical studies of the authors have shown that the IM $S_{a,gm}(T_1,1.6T_1)$ does not reduce substantially the RTR dispersion of the collapse capacity of multi-story frame structures, because it does not consider higher mode effects. Thus, for the present study an alternative "averaged" IM, $S_{a,gm}(0.2T_1,1.6T_1)$, is proposed, where the lower considered average range starts at 20% of the fundamental period, i.e., $T^{(1)} = 0.2T_1$, to account for higher mode effects. This lower bound period is in accordance to with specifications of the Eurocode 8 (2004) and ASCE/SEI 41-06 (2007).

Subsequently, for the utilized IMs the standard deviation $\sigma_{\ln Sa}$,

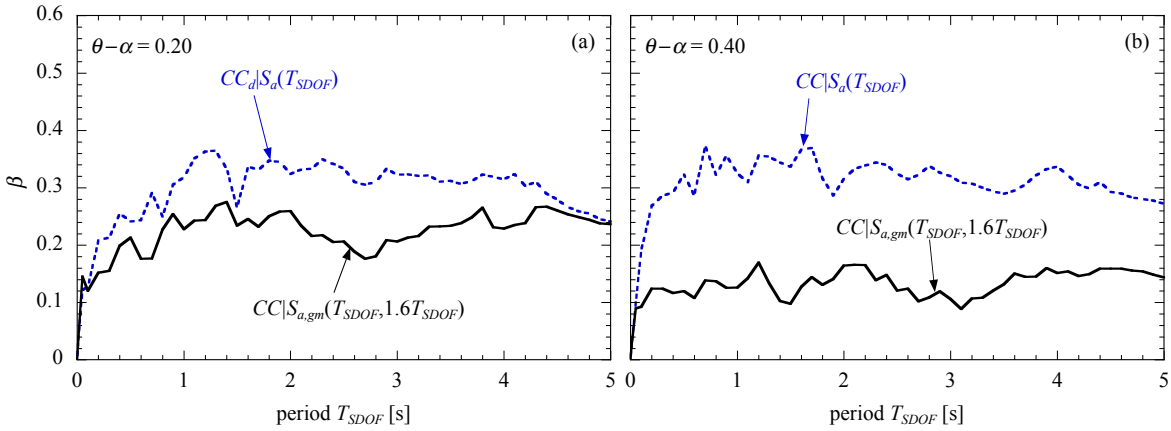

Figure 2. Dispersion measure β of the collapse capacity of SDOF systems for two IMs. Negative post-yield stiffness ratio as specified

$$\sigma_{\ln Sa} = \sqrt{\sum_{i=1}^{r} \frac{(\ln S_a^{(i)} - \mu_{\ln Sa})^2}{r-1}} \tag{6}$$

of the natural logarithm of $S_a^{(i)}$ with median $\mu_{\ln Sa}$ for the 44 ground motions (i.e., $r = 44$) of the FEMA P-695-FF record set as a function of the period T_{SDOF} is presented. The $S_a^{(i)}$, $i = 1,...,44$, are scaled according to the utilized IMs. In Figure 3 for each IM $\sigma_{\ln Sa}$ is graphically displayed. The arbitrary selected model frame exhibits a fundamental period $T_1 = 3.6$ s, and the elongated period $T_1^{P\Delta}$ due to the presence of gravity load is 3.82s. The second, third and fourth period with and without impact of gravity loads are also depicted. For IM $S_a(T_1)$ dispersion parameter $\sigma_{\ln Sa}$ becomes zero at T_1, for IM $S_a(T_1^{P\Delta})$ $\sigma_{\ln Sa}$ is zero at $T_1^{P\Delta}$, creating a narrow valley with small dispersion around the corresponding target periods. The "average" IM $S_{a,gm}(T_1,1.6T_1)$ leads to a wider valley of small $\sigma_{\ln Sa}$ values than IM $S_a(T_1)$, having a plateau of lower dispersion around to 1.3 times the period T_1. The IM $S_{a,gm}(0.2T_1,1.6T_1)$ leads to a broader plateau than IM $S_{a,gm}(T_1,1.6T_1)$. This IM yields in the higher mode domain to significantly smaller $\sigma_{\ln Sa}$ than the other three IMs, especially at the period of the second mode. The $\sigma_{\ln Sa}$ values of the unscaled records are also illustrated.

EVALUATION OF THE RECORD-TO-RECORD VARIABILITY OF THE COLLAPSE CAPACITY

Underlying set of generic frame structures

In this study different sets of generic multi-story frame structures are used to assess the RTR dispersion of the seismic collapse capacity that are similar to the ones described in Medina and Krawinkler (2003). All stories of the considered moment-resisting single-bay frame structures of N stories are of uniform height h, and they are composed of rigid beams and elastic flexible columns. According to the weak beam-strong column design philosophy inelastic rotational springs are located at both ends of the beams and at the base. To these springs, which exhibit a bilinear backbone curve, a non-degrading bilinear cyclic model is assigned. The strength of the springs is tuned such that yielding is initiated simultaneously at all spring locations in a static pushover analysis (without gravity loads) based on a first mode design load pattern. To each joint of the frames an identical lumped mass $m_i / 2 = m_s / 2$, $i = 1, ..., N$, is assigned. The bending stiffness of the columns and the initial stiffness of the springs are tuned to render a straight-line fundamental mode shape. Identical gravity loads are assigned to each story to simulate P-delta effects. This implies that axial column forces due to gravity increase linearly from the top to the bottom of each frame. Mass and current stiffness proportional 5% Rayleigh damping is used for the first mode and that mode at which the sum of nodal masses exceeds 95% of the total mass.

RTR variability of the collapse capacity of P-delta vulnerable MDOF systems is primarily influenced by

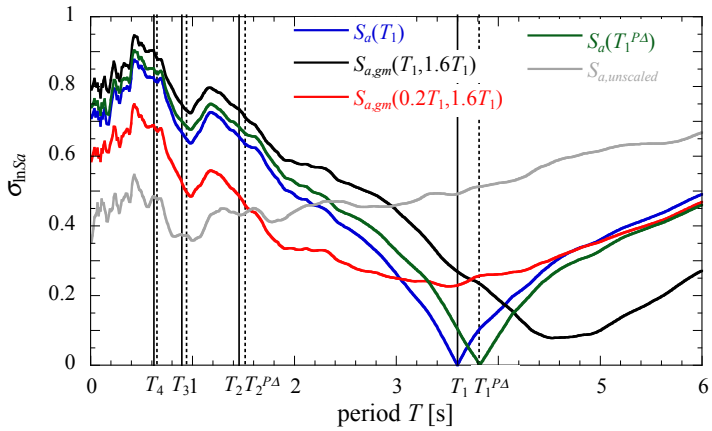

Figure 3. Dispersion spectra of scaled and unscaled spectral pseudo-accelerations of the 44 records of the FEMA P-695-FF records

- the fundamental period T_1 (without gravity loads),
- the effect of gravity loads on the fundamental period, i.e. $T_1^{P\Delta}$,
- the negative slope of the post-yield stiffness $\theta_i - \alpha_S$ in the capacity curve,
- the period elongation due to inelastic deformations, and thus on the degree of inelastic deformations,
- higher modes, correlated with the number of stories N and the structural periods.

In this study the elastic fundamental period T_1, the negative post-yield stiffness ratio $\theta_i - \alpha_S$, and the number of stories N serve as variables. Variation of these parameters affects period $T_1^{P\Delta}$ that is separately specified for each considered frame structure. The period elongation at collapse is largely controlled through $\theta_i - \alpha_S$, and thus not explicitly varied.

Note that IMs $S_a(T_1)$ and $S_a(T_1^{P\Delta})$, respectively, directly address the impact of periods T_1 and $T_1^{P\Delta}$, respectively, on the collapse dispersion. The "average" IM $S_{a,gm}(T_1,1.6T_1)$ captures additionally the effect of $\theta_i - \alpha_S$ and period elongation, and IM $S_{a,gm}(0.2T_1,1.6T_1)$ accounts also for the higher mode effects.

Three sets of generic frames are generated varying one of these aforementioned parameters and keeping the other two constant, isolating its contribution to the dispersion fluctuation for each considered IM. The parameters of each considered frame are listed in Table 1. An 18-story moment resisting frame with T_1 = 3.6 s and $\theta_i - \alpha_S$ = 0.20 is selected as the base-case system configuration. The corresponding non-dimensional pushover curves are depicted in Figure 4. In these curves base shear V and roof displacement x_N, respectively, is normalized with respect to the base shear at yield V_{y_ref} and the yield roof displacement x_{Ny_ref}, respectively, of the 18-story base-case frame.

The first set of frames includes the base-case frame with $\theta_i - \alpha_S$ = 0.20, and three similar structures with ratios $\theta_i - \alpha_S$ = 0.06, 0.10 and 0.40. Figure 4a shows the pushover curves in presence of gravity load for these frames and the base-case system. Larger values of $\theta_i - \alpha_S$ correspond to steeper negative post-yield slopes. Moreover, with increasing negative post-yield stiffness ratio a small decrease of the elastic slope and a reduction of the yield strength is observed.

Table 1. Three sets of generic frames: parameter variation

First set: $T_1 = 3.6s$, $N = 18$				Second set: $N = 18$, $\theta_i - \alpha_s = 0.20$				Third set: $T_1 = 3.6s$, $\theta_i - \alpha_s = 0.20$			
ID no.	$\theta_i - \alpha_S$	$T_1^{P\Delta} / T_1$	T_2 / T_1	ID no.	T_1 [s]	$T_1^{P\Delta} / T_1$	T_2 / T_1	ID no.	N	$T_1^{P\Delta} / T_1$	T_2 / T_1
1	0.06	1.029	0.404	1	0.9	1.046	0.403	1	1	1.141	
2	0.10	1.034	0.404	2	1.8	1.046	0.404	2	3	1.133	0.335
3	**0.20**	**1.045**	**0.404**	3	2.4	1.046	0.404	3	6	1.091	0.38
4	0.40	1.061	0.404	4	3.0	1.045	0.404	4	9	1.069	0.394
				5	**3.6**	**1.045**	**0.404**	5	12	1.058	0.399
				6	4.8	1.045	0.404	6	15	1.050	0.402
								7	**18**	**1.045**	**0.404**
								8	24	1.039	0.406

The second set consists of six frames with fundamental periods T_1 = 0.9 s, 1.8 s, 2.4 s, 3.0 s, 3.6 s and 4.8 s. All systems have 18 stories and a uniform negative post-yield stiffness ratio $\theta_i - \alpha_S$ = 0.20. The pushover curves for all frames of this set are depicted in Figure 4b. As the systems become more flexible, pushover curves shift to the right and the potential of inelastic deformations increases. The ratio of post-yield stiffness to elastic stiffness is constant, however, the system with the smallest fundamental period, i.e. T_1 = 0.9 s, exhibits the steepest slope since its elastic stiffness is larger.

In the third set the number of stories N is varied, creating frames with 1, 3, 6, 9, 12, 15, 18 and 24 stories. All systems have T_1 = 3.6 s and $\theta_i - \alpha_S$ = 0.20. Figure 4c shows that with increasing number of stories the yield-strength becomes larger. In absence of gravity loads all post-yield branches are in parallel, since all systems have the same elastic period and the same global strain hardening coefficient of 3%, i.e., $\alpha_S = 0.03$. It is noted that for the 3-story frame two modes are needed to exceed 95% of total mass, and the contribution of the first mode is 86%. For the 6 and 9-story frames, three modes are needed, and the contribution of first mode is 78%. Correspondingly, for the set of 12-, 15- and 18-story frames and for the 24-story frame, respectively, the effective total mass of four and five modes, respectively, exceed 95% of total, mass and the mass that correspond to first mode is 78% and 77%, respectively, of total mass.

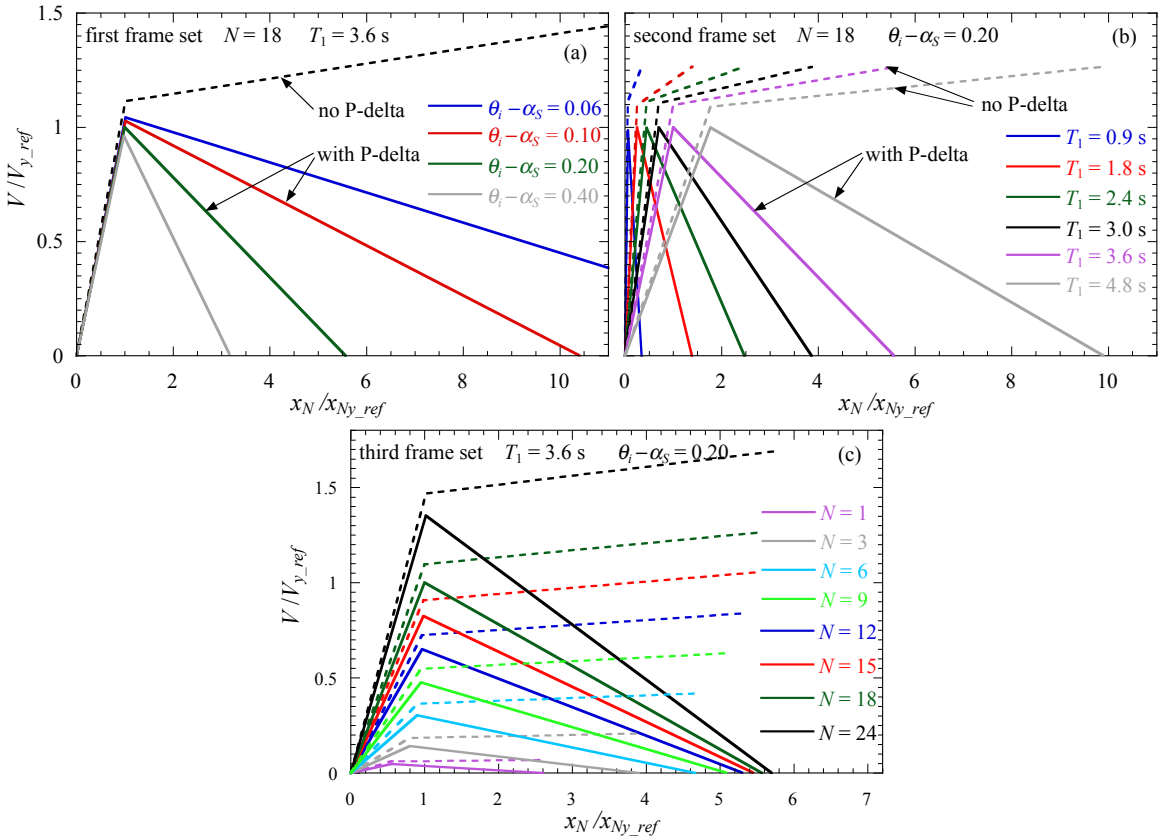

Figure 4. Global pushover curves for the frames of the (a) first set, (b) second set, and (c) third set. Dashed and solid lines represent systems with and without P-delta effects, respectively

Record-to-record variability of the collapse capacity with respect to the intensity measure

For each frame of the three sets IDAs were performed up to collapse for each of the 44 far-field ground motions of the FEMA P-695-FF set separately. Subsequently, for each structural configuration and each IM the RTR variability β according to Equation 2 was obtained.

The results for the first frame set are presented in Table 2 and Figure 5 for the four frames with different $\theta_i - \alpha_S$ ratios. It is observed that the dispersion of the collapse capacity decreases with increasing $\theta_i - \alpha_S$ values, because the structure becomes more brittle, and thus, the collapse potential increases. For instance, for the frame with $\theta_i - \alpha_S$ = 0.06 and IM $S_a(T_1)$ dispersion β is 0.542, while

for the combination $\theta_i - \alpha_S = 0.40$ and IM $S_a(T_1)$ the corresponding outcome is $\beta = 0.387$. The difference of the collapse variability β based on IM $S_a(T_1^{P\Delta})$ and IM $S_a(T_1)$ is negligible for 18-story structure with different negative post-yield stiffness ratio $\theta_i - \alpha_S$ of 0.06, 0.10, 0.20, and 0.40. For small negative post-yield stiffness ratios $\theta_i - \alpha_S$ of 0.06 and 0.10, the average IM $S_{a,gm}(T_1,1.6T_1)$ leads to smaller dispersion β than the single target spectral based on IM $S_a(T_1)$, but for large $\theta_i - \alpha_S$ values to a slightly larger collapse dispersion. The IM $S_{a,gm}(0.2T_1,1.6T_1)$ results in the smallest dispersion for all considered frames of this set. Compared with the outcomes for IM $S_a(T_1)$ the RTR variability decreases up to 20%.

Table 2. Dispersion of the collapse capacity for the four frames of the first set

First set: $T_1 = 3.6$ s, $N = 18$					
Set characteristics		Standard deviation β of the collapse capacity based on different IMs			
ID no.	$\theta_i - \alpha_S$	$S_a(T_1)$	$S_a(T_1^{P\Delta})$	$S_{a,gm}(T_1,1.6T_1)$	$S_{a,gm}(0.2T_1,1.6T_1)$
1	0.06	0.542	0.544	0.527	0.492
2	0.10	0.508	0.507	0.485	0.445
3	**0.20**	**0.413**	**0.410**	**0.416**	**0.339**
4	0.40	0.387	0.382	0.404	0.307

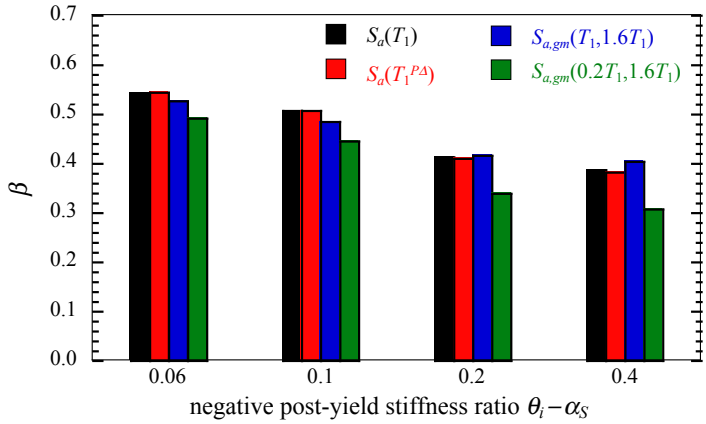

Figure 5. Dispersion of the collapse capacity for the four frames of the first set. IMs as specified

For the second set, collapse capacity dispersion due to RTR variability increases for systems with longer fundamental periods, see Table 3 and Figure 6. The dispersion grows from 0.339 to 0.499, when the fundamental period T_1 increases from 0.9 s to 4.8 s, since the potential of inelastic deformations increases as the system becomes more flexible. For structures with fundamental periods T_1 up to 3.0 s, dispersion β based on IM $S_a(T_1^{P\Delta})$ is slightly smaller than the outcome based in IM $S_a(T_1)$. Similarly, the average IM $S_{a,gm}(T_1,1.6T_1)$ leads to smaller β than the single target spectral based IM $S_a(T_1)$ for the frames in the range $0.9\,\text{s} \le T_1 \le 3.0\,\text{s}$, and considerably larger RTR collapse variability for the flexible system with $T_1 = 4.8$ s. Again, the average IM $S_{a,gm}(0.2T_1,1.6T_1)$ yields the smallest dispersion for all the six structural configurations with various fundamental periods T_1 of the 18-story frames with $\theta_i - \alpha_S = 0.20$. The reduction compared to β based on IM $S_a(T_1)$ is on average about 20% with its peak value of decrease of 30% for $T_1 = 3.0$ s.

Table 3. Dispersion of the collapse capacity for the six frames of the second set

Second set: $N = 18$, $\theta_i - \alpha_s = 0.20$					
Set characteristics		Standard deviation β of the collapse capacity based on different IMs			
ID no.	T_1 [s]	$S_a(T_1)$	$S_a(T_1^{P\Delta})$	$S_{a,gm}(T_1,1.6T_1)$	$S_{a,gm}(0.2T_1,1.6T_1)$
1	0.9	0.339	0.330	0.273	0.266
2	1.8	0.363	0.354	0.298	0.274
3	2.4	0.395	0.375	0.331	0.326
4	3.0	0.422	0.412	0.377	0.294
5	**3.6**	**0.413**	**0.410**	**0.416**	**0.339**
6	4.8	0.499	0.501	0.535	0.445

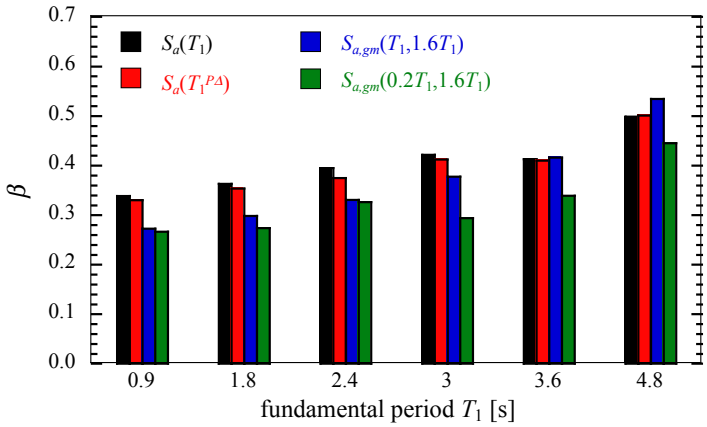

Figure 6. Dispersion of the collapse capacity for the six frames of the second set. IMs as specified

Results of the third set reveal that, as the number of stories increases from one to twelve, the RTR collapse capacity uncertainty increases for IM $S_a(T_1)$ from 0.262 to 0.423, compare with Table 4 and Figure 7. A further increase of the number of stories, however, does not increase the dispersion. For instance, for the 24-story frame based on IM $S_a(T_1)$ dispersion β is 0.405. For the one-story system, IMs of $S_{a,gm}(T_1,1.6T_1)$ and $S_a(T_1^{P\Delta})$ yields a reduced RTR variability of 30% and 10%, respectively, compared to the conventional $S_a(T_1)$. Actually, for the one-story frame the IM $S_{a,gm}(T_1,1.6T_1)$ gives the smallest collapse capacity dispersion of all frames of the three sets. Furthermore, it is the only structural configuration, where IMs $S_a(T_1)$ and $S_a(T_1^{P\Delta})$ lead to completely different dispersion predictions. This can be attributed to the fact that for multi-story frames the elastic stability θ_e is smaller than the inelastic stability θ_i, as visualized in Figure 1. In contrast, a one-story frame with a SDOF exhibits only one stability coefficient θ uniform in both elastic and post-yield branches of deformation (MacRae, 1994). This "global" stability coefficient θ is of the same order as the inelastic stability coefficient θ_i of the multi-story frames. In the one-story frame the period elongation due to P-delta is associated with the θ, and is, thus, larger than the corresponding elongation of a multi-story frame associated with the elastic stability coefficient $\theta_e(\ll\theta_i)$. Therefore, for the one-story frame the target spectral acceleration $S_a(T_1^{P\Delta})$ based on the period T differs from $S_a(T_1)$ based on the period considering gravity loads, $T^{P\Delta}$, by 14% if $\theta = 0.20$. Moreover, since an SDOF system does not exhibit any higher mode effects, the larger standard deviation of $\sigma_{\ln Sa}$ in the higher mode range (compare with Figure 3) does not contribute to the total RTR variability. It is noted, however, that already for the three-story building the superior performance of IM $S_{a,gm}(T_1,1.6T_1)$ over IM $S_a(T_1)$ is drastically reduced, compared to the one-story frame. Further increase of the story number diminishes or even reverses the positive effect of this average IM for the collapse dispersion. In contrast, using average IM $S_{a,gm}(0.2T_1,1.6T_1)$, which considers also higher mode effects, instead of IM $S_a(T_1)$ leads to a decrease of the dispersion of 20% even for the three-story frame. The use of IM $S_{a,gm}(0.2T_1,1.6T_1)$ again leads to the smallest collapse capacity dispersion β for all structural configurations, except for the one-story frame. The reduction of β based on IM $S_{a,gm}(0.2T_1,1.6T_1)$ compared to β based on $S_a(T_1)$ is on average about 18%.

Table 4. Dispersion of the collapse capacity for the eight frames of the third set

Third set: $T_1 = 3.6$ s, $\theta_i - \alpha_s = 0.20$					
Set characteristics		Standard deviation β of the collapse capacity based on different IMs			
ID no.	N	$S_a(T_1)$	$S_a(T_1^{P\Delta})$	$S_{a,gm}(T_1,1.6T_1)$	$S_{a,gm}(0.2T_1,1.6T_1)$
1	1	0.262	0.236	0.182	0.270
2	3	0.335	0.332	0.310	0.271
3	6	0.376	0.376	0.374	0.307
4	9	0.422	0.417	0.423	0.355
5	12	0.423	0.424	0.432	0.350
6	15	0.422	0.418	0.424	0.346
7	**18**	**0.413**	**0.410**	**0.416**	**0.339**
8	24	0.405	0.407	0.414	0.333

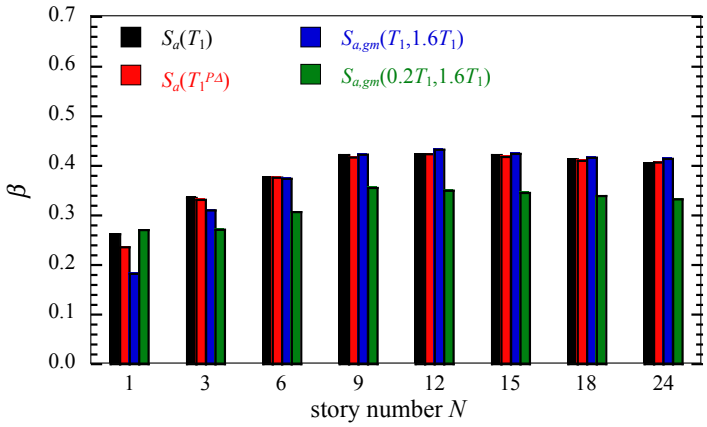

Figure 7. Dispersion of the collapse capacity for the eight frames of the third set. IMs as specified

Record-to-record variability of the collapse capacity with respect to code based intensity measures

In a further step recommendations provided in Eurocode 8 (2004), NZSEE (2006) and ASCE/SEI 41-06 (2007) are evaluated, referring to the selection and modification of the earthquake records with respect to the elongated period range, as well as higher mode effects. In these documents spectral matching period intervals of 0.2 T_1 - 2.0 T_1 (Eurocode 8, 2004), 0.4 T_1 - 1.5 T_1 (NZSEE, 2006) and 0.2 T_1 - 1.5 T_1 (ASCE/SEI 41-06, 2007) are proposed. Here, four flexible multi-story test structures with more "realistic" combinations between the number of stories N, the fundamental period T_1, and the negative global post-yield stiffness ratio $\theta_i - \alpha_S$ (see the first three columns of Table 5) are considered. All three parameters vary on a case-by-case basis, and as the number of stories increases, the systems have longer periods and exhibit larger values of negative post-yield stiffness. The corresponding dispersion of the collapse capacity of these structures for the four IMs used in the previous part and the three code-based IMs are listed in the second and third set of columns, respectively, as observed in Figure 8. The results of first set (4th to 7th column) are based on the two single target spectral IMs $S_a(T_1)$, $S_a(T_1^{P\Delta})$ and the two "average" IMs $S_{a,gm}(T_1,1.6T_1)$, $S_{a,gm}(0.2T_1,1.6T_1)$. The second set of code-based IMs (8th to 10th column) contains three "average" IMs with different period ranges, i.e., $S_{a,gm}(0.2T_1,1.5T_1)$ (ASCE/SEI 41-06, 2007), $S_{a,gm}(0.4T_1,1.5T_1)$ (NZSEE, 2006) and $S_{a,gm}(0.2T_1,2.0T_1)$ (Eurocode 8, 2004).

It is observed that with increasing negative post yield-stiffness ratio the systems become more vulnerable to the P-delta effect, and thus, leading to smaller collapse capacity dispersions. Similar trends have been observed in the previous part of this study studying three sets of generic frames. The single target spectral based IMs, $S_a(T_1)$ and $S_a(T_1^{P\Delta})$, result in larger RTR collapse capacity variability compared to the "average" proposed and code-based IMs. The superiority of "average" IMs, which take into account not only the period elongation, but also higher mode effects, is evident.

The fluctuation of collapse capacity uncertainty for the three code-based IMs is for the considered structures not larger than 9%. However, the EC8-based IM leads to smaller β for the 15- and 18-story frame, the difference for the 21-story frame is negligible, and the ASCE-based IM resulted in a lower dispersion for the 24-story frame. The NZSEE-based IM yields in general to larger dispersion of the average IMs, because the ratios for the considered systems of the fundamental period to the period of second, third and fourth mode are 0.4, 0.25 and 0.17, respectively.

CONCLUSIONS

This research evaluates different intensity measures (IMs) of generic moment-resisting frames vulnerable to the P-delta effect. A parametric study is carried out considering four IMs and three sets of generic frames. The first two IMs are single target spectral IMs: the 5% damped spectral pseudo-acceleration, $S_a(T_1)$ and $S_a(T_1^{P\Delta})$ at the elastic fundamental period without and with considering gravity loads, T_1 and $T_1^{P\Delta}$, respectively. In addition, there are two "average" IMs based on the geometric mean of the spectral pseudo-acceleration over a certain period range, $S_{a,gm}(T_1,1.6T_1)$ and

$S_{a,gm}(0.2T_1,1.6T_1)$. The latter three IMs take into account the period elongation, and the average IMs also consider higher mode effects. The fundamental period T_1, the negative post-yield stiffness ratio $\theta_i - \alpha_S$, and the number of stories N are the dominant structural parameters that affect significantly the RTR variability of the seismic collapse capacity of the considered structures vulnerable to P-delta. Therefore, in the present study they serve as variables. Three generic sets of frames have been derived varying one of these parameters and keeping the other two constant, isolating its contribution to the dispersion of the collapse capacities for each considered IM.

- In the first set of frames, the RTR variability of the collapse capacity of an 18-story frame with a period of 3.6 s was derived for four different post-yield negative slopes $\theta_i - \alpha_S = 0.06$, 0.10, 0.20 and 0.40. It is observed that a larger $\theta_i - \alpha_S$ leads to smaller dispersion, since as $\theta_i - \alpha_S$ increases the system becomes more vulnerable to the P-delta effect.
- The second set contains six different 18-story frames with $\theta_i - \alpha_S = 0.20$ and periods $T_1 = 0.9$ s, 1.8 s, 2.4 s, 3.0 s, 3.6 s and 4.8 s. Analyses based on IM $S_a(T_1)$ show that the collapse capacity dispersion due to RTR variability increases with increasing fundamental period. In particular, the dispersion increases from 0.339 to 0.499 as the fundamental period increases from 0.9 to 4.8 s.
- The third set includes eight frames with varying number of stories $N = 1$, 3, 6, 9, 12, 15, 18 and 24, and fixed parameters $T_1 = 3.6$ s and $\theta_i - \alpha_S = 0.20$. As the number of stories increases from 1 to 12, the collapse capacity dispersion based on IM $S_a(T_1)$ increases from 0.262 to 0.423, and stays relatively constant for structures with more stories.
- The choice of $S_{a,gm}(0.2T_1,1.6T_1)$ as an average IM results in the smallest dispersion for all frames of all the three sets, with the exception of a one-story frame with a single-degree-of-freedom SDOF). Since a SDOF structure does not exhibit higher modes, an "averaged" IM including spectral accelerations with periods below the elastic system period leads to a significant increase of the collapse dispersion. From this result it can be concluded that an equivalent SDOF system cannot reflect directly the collapse capacity dispersion of a multi-story building.

Subsequently, the RTR collapse capacity dispersion is evaluated for a fourth set of frames with more "realistic" combinations between the number of stories, the fundamental period and the negative global post-yield stiffness ratio. Three additional "average" code-based IMs on the collapse dispersion are considered, including different period ranges for determining the geometric mean of the spectral

Table 5. Dispersion of the collapse capacity for four test structures

Frame characteristics			Standard deviation β of the collapse capacity based on different IMs						
			IMs proposed in the present study				Code-based IMs		
N	T_1 [s]	$\theta_i - \alpha_S$	$S_a(T_1)$	$S_a(T_1^{P\Delta})$	$S_{a,gm}$ $(T_1,1.6T_1)$	$S_{a,gm}$ $(0.2T_1,1.6T_1)$	$S_{a,gm}$ $(0.2T_1,1.5T_1)$ (ASCE)	$S_{a,gm}$ $(0.4T_1,1.5T_1)$ (NZSEE)	$S_{a,gm}$ $(0.2T_1,2.0T_1)$ (EC8)
15	3.0	0.078	0.528	0.526	0.478	0.429	0.423	0.434	0.396
18	3.6	0.153	0.427	0.426	0.428	0.364	0.370	0.377	0.351
21	4.2	0.260	0.360	0.366	0.413	0.300	0.301	0.308	0.304
24	4.8	0.394	0.338	0.362	0.401	0.256	0.263	0.272	0.272

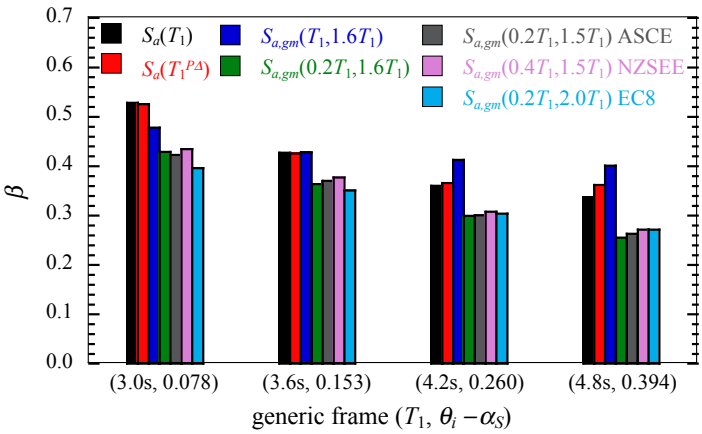

Figure 8. Dispersion of the collapse capacity for four test structures and seven IMs

pseudo-acceleration of 0.2 T_1 - 2.0 T_1, 0.4 T_1 - 1.5 T_1 and 0.2 T_1 - 1.5 T_1, respectively.

- Also for this frame set, the superiority of "average" IMs that take into account not only the period elongation but also the higher mode effects is evident.
- For all the four frames of this set the fluctuation of collapse capacity uncertainty based on the three code-based IMs is not larger than 9%.

REFERENCES

Adam C, Jäger C (2012) "Simplified collapse capacity assessment of earthquake excited regular frame structures vulnerable to P-delta", *Engineering Structures*, 44: 159-173

ASCE/SEI 41-06 (2007) Seismic Rehabilitation of Existing Buildings, American Society of Civil Engineers, Reston, Virginia, USA

Baker JW, Cornell CA (2005) "A vector-valued ground motion intensity measure consisting of spectral acceleration and epsilon", *Earthquake Engineering and Structural Dynamics*, 34: 1193-1217

Baker JW, Cornel CA (2006) "Spectral shape, epsilon and record selection", *Earthquake Engineering and Structural Dynamics*, 35: 1077-1095

Bianchini M, Diotallevi P, Baker, JW (2009) "Prediction of inelastic structural response using an average of spectral accelerations", *Proceedings of the 10th International Conference on Structural Safety and Reliability (ICOSSAR 09)*, Osaka, Japan, 13-19 September, 8 pp.

Cordova PP, Deierlein GG, Mehanny SSF, Cornell CA (2001) "Development of two-parameter seismic intensity measure and probabilistic assessment procedure", *Proceedings of the Second U.S.-Japan Workshop on Performance-based Earthquake Engineering Methodology for Reinforced Concrete Buildings Structures*, Sapporo, Japan, pp. 187-206

Eurocode 8 (2004) "Design provisions of structures for earthquake resistance", Part 1: General rules, seismic actions and rules for buildings

FEMA P-695 (2009) Quantification of building seismic performance factors, Federal Emergency Management Agency, Federal Emergency Management Agency, Washington DC

FEMA-350 (2000) Recommended seismic design criteria for new steel moment-frame buildings, Report No. FEMA-350, SAC Joint Venture, Federal Emergency Management Agency, Washington DC

Haselton CB (2009) Evaluation of ground motion selection and modification methods: predicting median interstory drift response of buildings, PEER Report 2009/01, Pacific Earthquake Engineering Research Center, College of Engineering, University of California, Berkeley

Ibarra L, Krawinkler H (2011) Variance of collapse capacity of SDOF systems under earthquake excitations. *Earthquake Engineering and Structural Dynamics*, 40: 1299-1314

Jalayer F, Beck JL, Zareian F (2012) "Information-based relative sufficiency of some ground motion intensity measures", *Proceedings of the 15th World Conference on Earthquake Engineering (15 WCEE 2012)*, Lisbon, Portugal, September 24-28, digital paper, paper no 5176, 10 pp.

Kadas K, Yakut A, Kazaz I (2011) "Spectral ground motion intensity based on capacity and period elongation", *Journal of Structural Engineering*, 137: 401-409

Krawinkler H, Zareian F, Lignos DG, Ibarra LF (2009) "Prediction of collapse of structures under earthquake excitations", *Proceedings of the 2nd International Conference on Computational Methods in Structural Dynamics and Earthquake Engineering (COMPDYN 2009)*, Rhodes, Greece, June 22-24, (Papadrakakis M, Lagaros ND, Fragiadakis M, eds), CD-ROM paper, paper no. CD449

Luco N, Cornell CA (2007) "Structure-specific scalar intensity measure for near-source and ordinary earthquake motions", *Earthquake Spectra*, 23: 357-391

MacRae GA (1994) "P-Δ effects on single-degree-of-freedom structures in earthquakes", *Earthquake Spectra*, 10: 539-568

Medina, RA, Krawinkler H (2003) Seismic demands for nondeteriorating frame structures and their dependence on ground motions, Report No. 144. The John A. Blume Earthquake Engineering Research Center, Department of Civil and Environmental Engineering, Stanford University, Stanford, CA

NZSEE (2006) "Assessment and improvement of the structural performance of buildings in earthquake", Recommendations of a NZSEE study Group on Earthquake Risk Buildings. New Zealand Society for Earthquake Engineering, New Zealand

Shome N, Cornell CA (1999) Probabilistic seismic demand analysis of nonlinear structures, RMS Tech Report No. 38. The John A. Blume Earthquake Engineering Research Center, Department of Civil and Environmental Engineering, Stanford University, Stanford, CA

Tsantaki S, Adam C (2013) "Collapse capacity spectra based on an improved intensity measure", Proceedings of the 4th ECCOMAS Thematic Conference on Computational Methods in Structural Dynamics and Earthquake Engineering (COMPDYN 2013), Kos Island, Greece, June 12-14, (Papadrakakis M, Papadopoulos V, Plevris V, eds), CD-ROM paper, paper no. 1382, 14 pp.